

2018

Effect of Fin Geometries on Condensation Heat Transfer and Pressure Drop inside Horizontal Small-Diameter 4 mm Microfin Tubes

Norihiro Inoue

Tokyo University of Marine Science and Technology, Japan, inoue@kaiyodai.ac.jp

Masataka Hirose

Graduate School of Marine Science and Technology, Tokyo University of Marine Science and Technology, d162016@edu.kaiyodai.ac.jp

Daisuke Jige

Tokyo University of Marine Science and Technology, Japan, djige00@kaiyodai.ac.jp

Follow this and additional works at: <https://docs.lib.purdue.edu/iracc>

Inoue, Norihiro; Hirose, Masataka; and Jige, Daisuke, "Effect of Fin Geometries on Condensation Heat Transfer and Pressure Drop inside Horizontal Small-Diameter 4 mm Microfin Tubes" (2018). *International Refrigeration and Air Conditioning Conference*. Paper 1996.

<https://docs.lib.purdue.edu/iracc/1996>

This document has been made available through Purdue e-Pubs, a service of the Purdue University Libraries. Please contact epubs@purdue.edu for additional information.

Complete proceedings may be acquired in print and on CD-ROM directly from the Ray W. Herrick Laboratories at <https://engineering.purdue.edu/Herrick/Events/orderlit.html>

Effect of Fin Geometries on Condensation Heat Transfer and Pressure Drop inside Horizontal Small-Diameter 4 mm Microfin Tubes

Norihiro INOUE^{1*}, Masataka HIROSE², Daisuke JIGE¹

¹ Tokyo University of Marine Science and Technology
Etchujima, Koto-ku, Tokyo, Japan
Phone number: +81-3-5245-7479, Fax number: +81-3-5245-7479,
E-mail address: inoue@kaiyodai.ac.jp, djige00@kaiyodai.ac.jp

² Graduate School of Marine Science and Technology,
Tokyo University of Marine Science and Technology,
Etchujima, Koto-ku, Tokyo, Japan

ABSTRACT

This study experimentally investigated the condensation heat transfer and pressure drop characteristics of R1234ze(E) inside horizontal small-diameter 4.0 mm OD microfin tubes having three different types of fin geometries. The specifications of the three fin geometries were 40 fins with a fin height of 0.18 mm and a helix angle of 18°, 50 fins with a fin height of 0.15 mm and a helix angle of 12°, and 50 fins with a fin height of 0.12 mm and a helix angle of 25°. The experiments were carried out for a range of mass velocities from 50 to 400 kgm⁻²s⁻¹, and at a saturation temperature of 35 °C. The effects of fin geometries such as the number of fins, fin height, and helix angle on the heat transfer and pressure drop were investigated. The heat transfer coefficient increased as the number of fins increased for the lowest mass velocity. Fin height was most effective on heat transfer enhancement at higher mass velocities. The heat transfer coefficient and pressure drop of the microfin tubes were compared with those of smooth tube and were evaluated in terms of the enhancement factor of heat transfer. The measured heat transfer coefficient and pressure drop were compared with previous correlations, and the results were verified practical effectiveness of the previous correlations for small-diameter microfin tubes.

1. INTRODUCTION

The energy demands of emerging countries are increasing as the economies of these countries develop; therefore, deterioration caused by global warming has become a concern. In developed and emerging economies, the demand for air conditioning is increasing along with the improvement in living standards. In the refrigeration and air-conditioning fields, microfin tubes with an outside diameter (OD) of 5 mm or less have been developed to enhance energy savings by improving the performance of the heat exchanger and by reducing the charge amount of the refrigerant by downsizing the heat exchanger. Microfin tubes with a 4 mm OD have been used in practical applications. However, with the decrease in the tube diameter, the frictional pressure drop increases. Therefore, it is important to investigate heat transfer characteristic at low mass velocity conditions. Moreover, hydrofluoroolefin (HFO) refrigerant is attracting attention as a low global warming potential (GWP) refrigerant, because regulation of hydrofluorocarbon (HFC) refrigerant is expected to become restrictive. For example, the Kigali amendment to the Montreal Protocol (MOP28) requires an 85% reduction of HFCs by 2036 in developed countries, and by 2047 in developing countries. Diani et al. (2017) investigated the condensation heat transfer coefficient and pressure drop of HFO refrigerant R1234yf in a microfin tube with 3.4 mm fin tip diameter. However, only a limited number of studies exist on condensation heat transfer with HFO refrigerants in small-diameter microfin tubes. In addition, it is necessary to validate the applicability of previous correlations to the condensation heat transfer coefficient and pressure drop of HFO refrigerants inside small-diameter microfin tubes.

In this study, the condensation heat transfer and frictional pressure drop characteristics of R1234ze(E) inside three kinds of horizontal microfin tubes of 4.0 mm outer diameter and a smooth tube with the same diameter with mass velocity range of 50–200 kgm⁻²s⁻¹ were investigated. We clarified the effects of fin geometries on condensation heat

transfer and pressure drop characteristics. Moreover, the heat transfer coefficient and frictional pressure drop of the microfin tubes were compared with those of the smooth tube, the enhancement factor of heat transfer was evaluated, and the measured heat transfer coefficient and pressure drop were compared with previous correlations. The results verified the practical effectiveness of the previous correlations for small-diameter microfin tubes.

2. EXPERIMENTAL APPARATUS AND PROCEDURE

Figure 1 shows a schematic diagram of the experimental apparatus, which is a vapor compression heat pump system. The refrigerant loop consists of a compressor, an oil separator, a pre-condenser, a test section, a rear condenser, a receiver, a mass flow meter, an expansion valve, and an evaporator. The refrigerant flow rate is adjusted by the expansion valve, bypass valve, and flow control valve. The flow rate of the refrigerant is measured using the Coriolis mass flow meter.

Figure 2 shows details of the pre-condenser and test section. The pre-condenser and test section are a double-tube heat exchanger. The test section consists of three sub-sections with 200 mm length. In each sub-section, a test tube is cooled by passing cooling water through the annulus, and the refrigerant flows within an inner tube. The measurement length of the pressure drop and the effective heat transfer length are 800 mm and 200 mm, respectively. The refrigerant temperatures are measured by K-type sheath thermocouples at the inlet of the pre-condenser, and inlet and outlet of the test section. The tube's outer wall temperatures are measured at the top and bottom and the center of each sub-section by T-type thermocouples. The refrigerant pressures at the inlet of the test section and the inlet of the pre-condenser are measured by absolute pressure transducers, and the refrigerant pressure drop between the inlet and outlet of the test tube is measured by two differential pressure transducers with full scales of 100 kPa and 20 kPa, respectively. The flow rates of the cooling water for the test section and pre-condenser are measured using the volumetric flowmeters. The bulk temperatures of the cooling water are measured by Pt-resistance thermometers inserted at the inlet and outlet of each sub-section and pre-condenser.

Table 1 summarizes the specifications of the test tubes and figure 3 shows the schematic view of the test microfin tube. The test copper tubes are the smooth tube and the three microfin tubes of outer diameter of 4.0 mm and equivalent inner diameter of 3.5 mm. Three kinds of the test microfin tubes were used, so that LF50L has 50 fins, with a fin height of 0.15 mm and helix angle of 12°, LF50S has 50 fins, with a fin height of 0.12 mm and helix angle of 25°, and HF40 has 40 fins, with a fin height of 0.18 mm and helix angle of 18°.

3. DATA REDUCTION

The condensation heat transfer coefficient α is defined as:

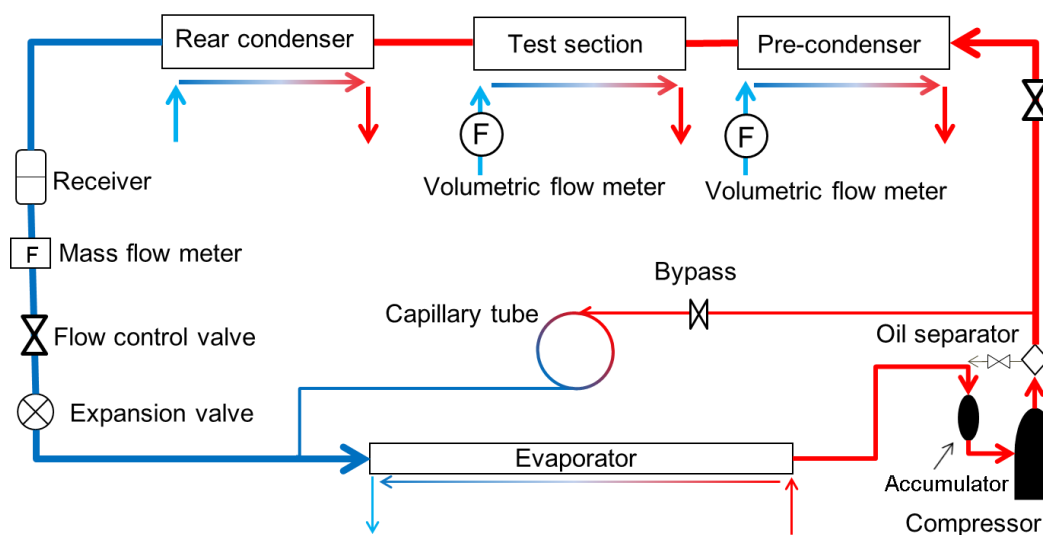


Figure 1: Schematic diagram of the experimental apparatus

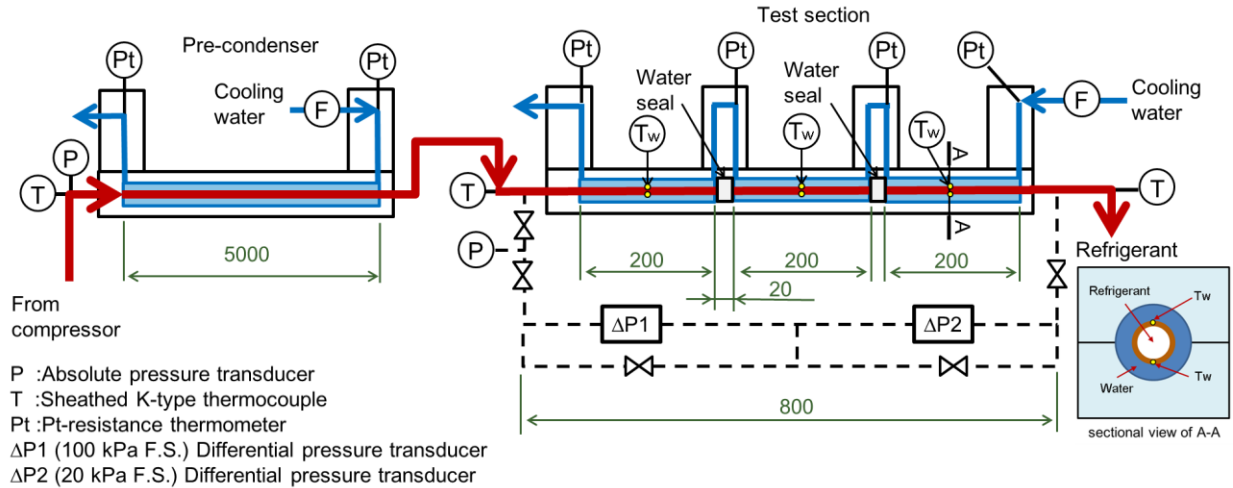


Figure 2: Details of the pre-condenser and test section

Table 1: Specifications of the test tubes

Tube type	Microfin			Smooth
Tube name	HF40	LF50S	LF50L	SM
Outside diameter d_o [mm]	4.03	4.00	4.00	4.00
Equivalent ID d_{eq} [mm]	3.48	3.46	3.44	3.48
Wall thickness δ [mm]	0.21	0.22	0.22	0.27
Fin height h [mm]	0.18	0.13	0.15	-
Helix angle θ [deg.]	17	25	12	-
Number of fins n [-]	40	50	50	-
Area enlargement ratio η [-]	2.13	1.90	1.94	1

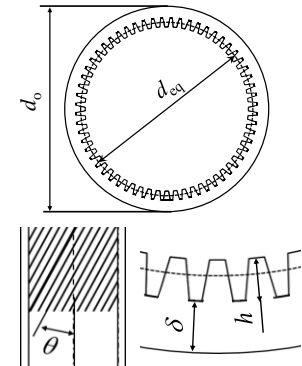


Figure 3: Schematic view of the test microfin tube.

$$\alpha = \frac{Q}{\pi d_{eq} L (T_{sat} - T_{wi})} \quad (1)$$

where Q is the heat transfer rate, L is the effective heat transfer length of the sub-section, and d_{eq} is the equivalent diameter of the test microfin tube. The equivalent inner diameter refers to the inner diameter of a smooth tube with the same internal free flow area as the test microfin tube. For the experiment using the smooth tube, d_{eq} is defined by the inner diameter. Q is calculated using isobaric specific heat, flow rate, and temperature difference of the cooling water flowing in the annulus of each sub-section. T_{sat} is the saturation temperature of the refrigerant from the measured refrigerant pressure. T_{wi} is the tube's inner wall temperature. T_{wi} is calculated from the measured tube's outer wall temperature considering one-dimensional steady heat conduction.

The frictional pressure drop during the condensation process ΔP_F is defined as follows:

$$\Delta P_F = \Delta P_T - \Delta P_M \quad (2)$$

where ΔP_T is the measured pressure drop and ΔP_M is the pressure drop due to momentum change calculated by a separated flow model. ΔP_M is defined as:

$$\Delta P_M = \Delta \left\{ \frac{G^2 x^2}{\xi \rho_V} + \frac{G^2 (1-x)^2}{(1-\xi) \rho_L} \right\} \quad (3)$$

ξ is a void fraction, G is the mass velocity, and x is the vapor quality. The physical properties of the refrigerant and cooling water, respectively, were calculated from REFPROP Ver. 9.1 (Lemmon et al. 2013). In the case of smooth tubes were used in the experiments, ξ could be estimated from Eq. (4) below, as proposed by Smith (1969).

$$\xi_{\text{Smith}} = \left[1 + \frac{\rho_V}{\rho_L} \left(\frac{1-x}{x} \right) \left(0.4 + 0.6 \sqrt{\frac{\frac{\rho_L + 0.4 \frac{1-x}{x}}{\rho_V}}{1 + 0.4 \frac{1-x}{x}}} \right) \right]^{-1} \quad (4)$$

In the case of microfin, ξ could be estimated from Eq. (5) below, as proposed by Koyama et al. (2001).

$$\xi = 0.81 \xi_{\text{Smith}} + 0.19 x^{100(\rho_V/\rho_L)^{0.8}} \left[1 + \frac{\rho_V}{\rho_L} \left(\frac{1-x}{x} \right) \right]^{-1} \quad (5)$$

4. EXPERIMENTAL RESULTS AND DISCUSSION

4.2 Condensation heat transfer

Figures 4(a) and (b) show the typical relation between the condensation heat transfer coefficient α and wetness $1-x$ in LF50L. The heat transfer coefficients of LF50L decrease with increasing wetness, because the thermal resistance of the condensate film increases in the condensation process. In addition, the heat transfer coefficients decrease due to the decreasing forced convection as the mass velocity decreases. For the HF40 and LF50S, the trends of heat transfer coefficients are similar to LF50L. The heat transfer coefficients of SM decrease with increasing wetness. However, the heat transfer coefficients are not affected by the mass velocity. It is considered that the smooth tube is dominated by free convection heat transfer not forced convection heat transfer.

Figures 5 (a) and (b) show the relation between the enhancement factor of heat transfer EF and wetness $1-x$ for mass velocities of 200 and 50 $\text{kg m}^{-2} \text{s}^{-1}$. The enhancement factor of heat transfer EF is defined as:

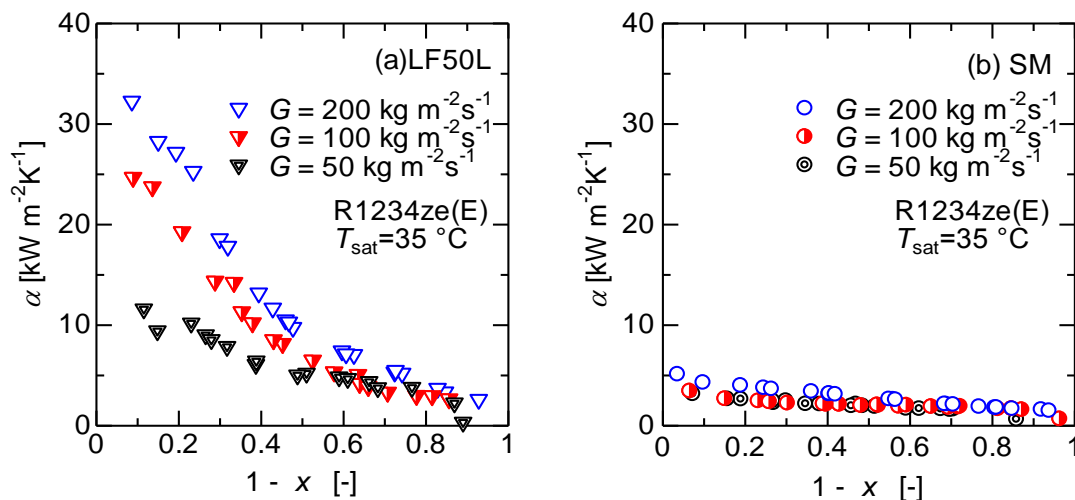


Figure 4: Typical relation between heat transfer coefficients and wetness.

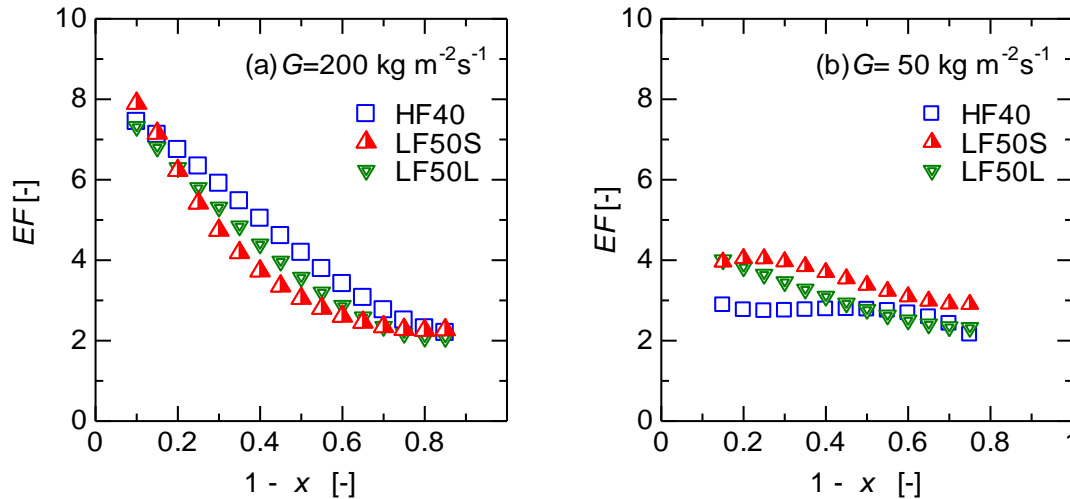


Figure 5: Relation between heat transfer enhancement factor and wetness.

$$EF = \frac{\alpha_{MF}}{\alpha_{SM}} \quad (6)$$

where α_{MF} is the heat transfer coefficient of the microfin tube, and α_{SM} is the heat transfer coefficient of the smooth tube SM. For mass velocity of $200 \text{ kg m}^{-2}\text{s}^{-1}$, the EF of both microfin tubes shows the largest value of 6 to 7 at the low wetness region. The EF gradually decreases with condensation, and it decreases to $EF \approx 2$, which is the same as the heat transfer area enlargement ratio η at a wetness of 0.8. The heat transfer of the microfin tubes is dominated by forced convection. In addition, thermal resistance decreased due to a thin liquid film formed on the fin tip by the surface tension, which enhances heat transfer and promotes a high heat transfer coefficient at the low wetness region for a mass velocity of $200 \text{ kg m}^{-2}\text{s}^{-1}$. For a mass velocity of $50 \text{ kg m}^{-2}\text{s}^{-1}$, the EF of each microfin tube showed a value of 2 to 4, and the values are larger than the heat transfer area enlargement ratio η . Comparing LF50S, LF50L, and HF40, the EF of HF40 is higher than those of LF50S and LF50L for a mass velocity of $200 \text{ kg m}^{-2}\text{s}^{-1}$ at the whole wetness region, whereas the EF of LF50S is higher than those of HF40 and LF50L for a mass velocity of $50 \text{ kg m}^{-2}\text{s}^{-1}$. The EF of LF50L for a mass velocity of $200 \text{ kg m}^{-2}\text{s}^{-1}$ is lower than that of HF40, and higher than that of LF50S. The EF of LF50L for a mass velocity of $50 \text{ kg m}^{-2}\text{s}^{-1}$ shows the same value as LF50S at the low wetness region; however, it shows the same value as HF40 at the high wetness region. In higher mass velocity conditions, the effect of fin height on the heat transfer is larger than that of the helix angle and number of fins at the middle wetness region. In low mass velocity conditions, the effect of the number of fins on heat transfer is larger than those of fin height and helix angle at the low wetness region, and the effect of helix angle on heat transfer is larger than those of fin height and number of fins at the middle to high wetness region.

4.2 Pressure drop

Figures 6(a) and (b) show the relation between the frictional pressure drop $\Delta P_f/\Delta Z$ and wetness $1-x$ in the microfin and smooth tubes for mass velocities of 200 and $100 \text{ kg m}^{-2}\text{s}^{-1}$. These figures also show the frictional pressure drops of LF50L, LF50S, HF40 and SM. The pressure drop decreases with decreasing mass velocity and increasing wetness. This is caused by the decrease in the vapor velocity and the wall shear stress during the condensation process. Comparing the microfin and smooth tubes, the pressure drops of all microfin tubes are 1.5 to 2.5 times higher than that of the smooth tube. Comparing the results for each microfin tube, there was not a significant difference of frictional pressure drop between LF50L, LF50S, and HF40. The fin height of HF40 is larger than that of LF50L and LF50S; however, the number of fins for HF40 is lower than those of LF50L and LF50S. In addition, the helix angle of LF50L is lower than those of HF40 and LF50S. It is considered that the effects of the fin geometries offset the characteristics of each other on the pressure drops; therefore, there are no differences in frictional pressure drop.

4.3 Comparison of the previous correlations for condensation heat transfer coefficients

Figures 7(a), (b), and (c) show the comparisons of the experimental values and the calculated values by previous correlations of condensation heat transfer for microfin tubes by Yonemoto and Koyama (2007), Cavallini et al.

(2009), and author et al. (2012, 2018), respectively. Yonemoto and Koyama's correlation was proposed for the microfin tubes with average inner diameters of 6.25 to 8.37 mm and the refrigerants R123, R22, and R134a. Cavallini et al.'s correlation was proposed for the microfin tubes with fin tip diameters of 5.95 to 14.18 mm and refrigerants R22, R134a, R410A, and others. The authors' correlation was proposed for the several kinds of 4 mm small-diameter microfin tubes based on HF40 with an equivalent diameter of 3.48 mm and the refrigerants R32, R410A, and R152a. The figures show that Yonemoto and Koyama's correlation had higher accuracy at the high wetness region, and Cavallini et al.'s correlation could not predict the heat transfer coefficients at the low wetness region. The authors' correlation could predict the heat transfer coefficients for refrigerant R1234ze(E) of HF40, LF50L, and LF50S. It follows that the authors' correlation can be applied to the heat transfer coefficients for several kinds of fin geometries with 4 mm small-diameter tubes.

4.4 Comparison of the previous correlations for pressure drops during condensation flow

Figures 8(a), (b), and (c) show a comparison of experimental values and the calculated values by previous correlations for microfin tubes by Cavallini et al. (1997), Yonemoto and Koyama (2007), and author et al. (2012, 2018), respectively. Cavallini et al.'s correlation was proposed for microfin tubes with fin tip diameters of 6.04 to 14.18 mm and refrigerants R22, R134a, R32, and others. The authors' correlation was proposed for the several kinds of 4 mm small-diameter smooth and microfin tubes based on SM and HF40 with equivalent diameter of 3.48 mm and refrigerants R32, R410A, and R152a. From the figures, all correlations are within approximately $\pm 30\%$. Cavallini et al.'s correlation slightly overestimates the frictional pressure drop at the low wetness region. Yonemoto and Koyama's and the author et al.'s correlations slightly underestimate the frictional pressure drop at the high wetness region.

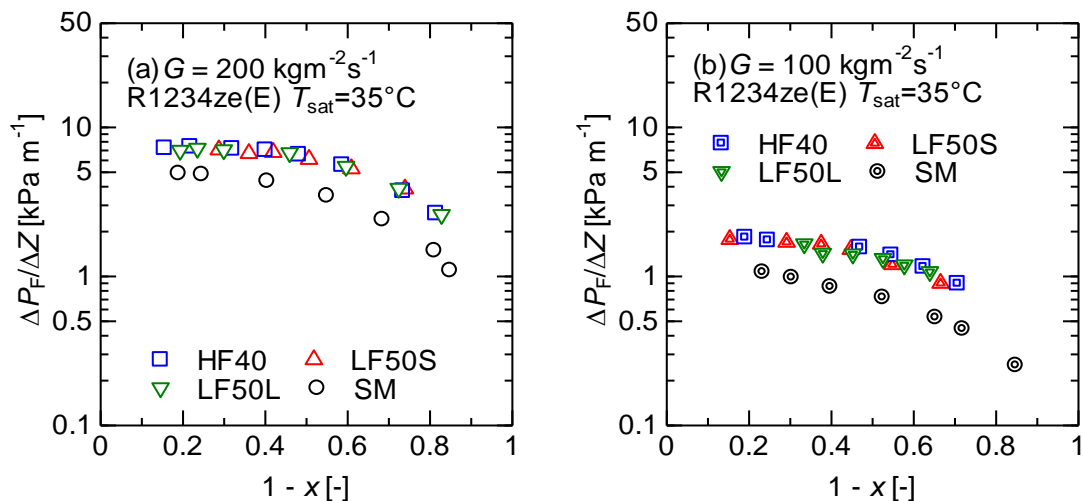


Figure 6: Relation between pressure drop and wetness.

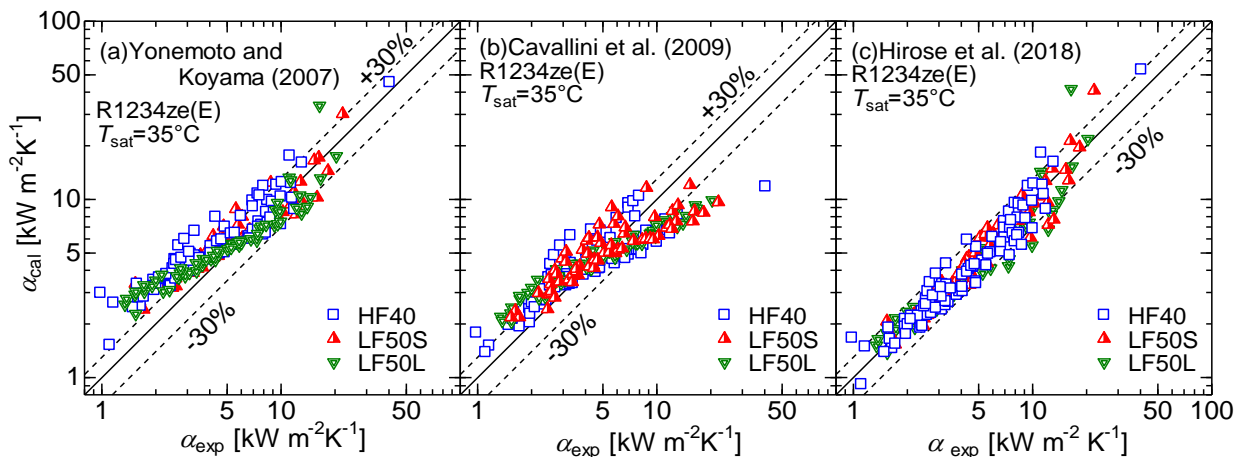


Figure 7: Comparison of the measured and predicted values for heat transfer coefficients in microfin tube.

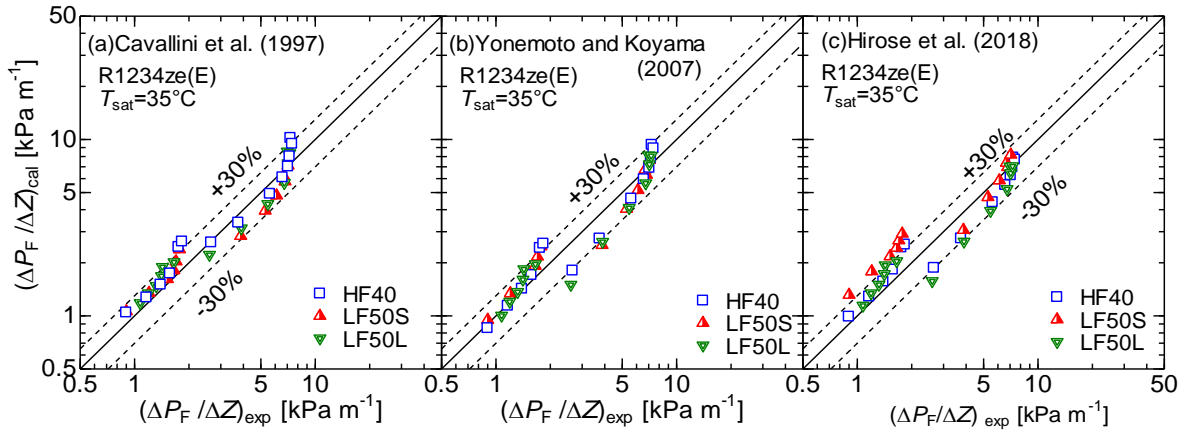


Figure8: Comparison of measured and predicted values for pressure drop in microfin tube.

5. CONCLUSIONS

The condensation heat transfer and frictional pressure drop characteristics of R1234ze(E) inside horizontal small-diameter microfin tubes and a smooth tube of 4.0 mm OD in the mass velocity range of 50–200 kgm⁻²s⁻¹ were investigated. The following results were obtained.

- The pressure drop decreases with decreasing mass velocity and increasing wetness. This is caused by the decrease in the vapor velocity and the wall shear stress in the condensation process. Comparing the results for each microfin tube, no significant difference was observed in the frictional pressure drop between LF50L, LF50S, and HF40.
- In higher mass velocity conditions, the effect of fin height on the heat transfer is larger than that of the helix angle and number of fins at the middle wetness region. In low mass velocity conditions, the effect of the number of fins on heat transfer is larger than those of fin height and helix angle at the low wetness region, and the effect of helix angle on heat transfer is larger than those of fin height and number of fins at middle to high wetness region.
- The authors' correlation can be applied to the heat transfer coefficients for several kinds of fin geometries with 4 mm small-diameter tubes. The authors' correlation, which was proposed for several kinds of 4-mm small-diameter smooth and microfin tubes, can be correlated within approximately $\pm 30\%$.

NOMENCLATURE

d	diameter	(m)
EF	enhancement factor	(-)
G	refrigerant mass velocity	(kg m ⁻² s ⁻¹)
h	Fin height	(m)
L	heat transfer length	(m)
m	flow rate	(kg s ⁻¹)
n	Number of fins	(-)
P	pressure	(Pa)
Q	heat transfer rate	(W)
T	temperature	(K)
x	vapor quality	(-)
Greek letters		
A	heat transfer coefficient	(W m ⁻² K ⁻¹)
δ	wall thickness	(m)

ΔP_T	total pressure drop	(Pa)
ΔP_F	frictional pressure drop	(Pa)
ΔP_M	pressure drop due to momentum change	(Pa)
θ	helix angle of fin	(degree)
μ	viscosity	(kg m ⁻¹ s ⁻¹)
ξ	void fraction	(-)
ρ	density	(kg m ⁻³)

Subscript

cal	calculate
eq	equivalent
exp	experiment
L	liquid
o	outside
sat	saturation
V	vapor
wi	inner wall surface
W	wall

REFERENCES

Cavallini A, Del Col D, Doretti L, Longo G.A, Rossetto L. Pressure Drop during Condensation and Vaporization of Refrigerants inside Enhanced Tubes, *Heat and Technology* 1997, 15, 3-10.

Cavallini A, Del Col D, Rossetto L, Mancin S. Condensation of Pure and Near-azeotropic Refrigerants in Microfin tubes A New Computational Procedure, *Int. J. Refrig.* 2009, 32, 162-174.

Diani A, Cavallini A, Rossetto L. R1234yf Condensation Inside a 3.4 mm ID Horizontal Microfin Tube, *Int. J. Refrig.* 2017, 75, 178-189.

Hirose M, Ichinose J, Inoue N, Development of the general correlation for condensation heat transfer and pressure drop inside horizontal 4 mm small-diameter smooth and microfin tubes, *Int. J. Refrig.* 2018, 90, 238-248.

Inoue N, Ichinose J. Single-phase Heat Transfer and Pressure Drop inside Internally Helical-grooved Horizontal Small-diameter Tubes, *Int. J. Air-Conditioning and Refrig.*, 2012; 20(4), DOI: 10.1142/S2010132512500228.

Koyama S, Chen Y, Kitano R, Kuwahara K. Experimental Study on Void Fraction of Two-phase Flow inside a Micro-fin tube, *The reports of IAMS, Kyushu Univ.* 2001, 15(1), 79-85.

Lemmon E.W, Huber M.L, McLinden M.O. NIST standard reference database 23, Reference Fluid Thermodynamic and Transport Properties REFPROP Ver. 9.1 2013; *National Institute of Standards and Technology*.

Smith SL. Void Fractions in Two-Phase Flow: A Correlation Based upon an Equal Velocity Head Model, *Proc. Instn Mech. Engrs.* 1969, 184(1)(36), 647-664.

Yonemoto R, Koyama S. Experimental Study on Condensation of Pure Refrigerants in Horizontal Micro-fin Tubes, Proposal of Correlations for Heat Transfer Coefficient and Frictional Pressure Drop, *Trans. JSRAE*, 2007, 24(2), 139-148, (in Japanese).

ACKNOWLEDGEMENT

This study was supported by the Research & Development Section, Technical Department, Kobelco & Material Copper Tube, LTD. We would like to express our gratitude for the support provided.